

This is the authors' version (pre peer-review) of the manuscript: N R. Rezende et al, Advanced Electronic Materials <https://doi.org/10.1002/aelm.201800591> , That has been published in its final form: <https://onlinelibrary.wiley.com/doi/abs/10.1002/aelm.201800591>

Probing the Electronic Properties of Monolayer MoS₂ via Interaction with Molecular Hydrogen

*Natália P. Rezende, Alisson R. Cadore, Andreij C. Gadelha, Cíntia L. Pereira, Vinicius Ornelas, Kenji Watanabe, Takashi Taniguchi, André S. Ferlauto, Ângelo Malachias, Leonardo C. Campos, and Rodrigo G. Lacerda**

N. P. Rezende, Dr. A. R. Cadore, A. C. Gadelha, C. L. Pereira, V. Ornelas, Prof. A. Malachias, Prof. L. C. Campos, Prof. R. G. Lacerda*

Departamento de Física, Universidade Federal de Minas Gerais, Belo Horizonte, 30123-970, Brasil

E-mail: rlacerda@fisica.ufmg.br

Prof. A. S. Ferlauto

Centro de Engenharia, Modelagem e Ciências Sociais Aplicadas, Universidade Federal do ABC, 09210580, Brasil

K. Watanabe, T. Taniguchi,

Advanced Materials Laboratory, National Institute for Materials Science, Namiki, 305-0044, Japan

Keywords: hydrogen detection, monolayer MoS₂, gas interaction, field effect transistors

This work presents a detailed experimental investigation of the interaction between molecular hydrogen (H₂) and monolayer MoS₂ field effect transistors (MoS₂ FET), aiming for sensing application. The MoS₂ FET exhibit a response to H₂ that covers a broad range of concentration (0.1-90 %) at a relatively low operating temperature range (300-473 K). Most important, H₂ sensors based on MoS₂ FETs show desirable properties such as full reversibility and absence of catalytic metal dopants (Pt or Pd). The experimental results indicate that the conductivity of MoS₂ monotonically increases as a function of the H₂ concentration due to a reversible charge transferring process. It is proposed that such process involves dissociative H₂ adsorption driven by interaction with sulfur vacancies in the MoS₂ surface (V_S). This description is in agreement with related density functional theory studies about H₂ adsorption on MoS₂. Finally, measurements on partially defect-passivated MoS₂ FETs using atomic layer deposited aluminum oxide consist of an experimental indication that the V_S plays an important role in the H₂ interaction with the MoS₂. These findings provide insights for futures applications in catalytic process between monolayer MoS₂ and H₂ and also introduce MoS₂ FETs as promising H₂ sensors.

1. Introduction

Molecular hydrogen (H₂) has great potential as a non-polluting source of energy used in several industrial applications. Especially it is used for desulphurization of petroleum products, synthesis of ammonia, methanol and as a green fuel in mobile applications such as cars and rockets.^[1] For these reasons, areas involving H₂ generation, storage and detection are under continuous development. In special, sensing of H₂ is crucial for safety applications due to its flammability range of 4.0-75.0 % by

This is the authors' version (pre peer-review) of the manuscript: N R. Rezende et al, Advanced Electronic Materials <https://doi.org/10.1002/aelm.201800591> , That has been published in its final form: <https://onlinelibrary.wiley.com/doi/abs/10.1002/aelm.201800591> volume in the air.^[1,2] Hence, it is indispensable to develop high-performance sensors with a wider measurement range (1-99% v/v H₂) to detect and monitor H₂ for industrial and safety applications.^[2] There are several commercially available hydrogen sensors classified by the sensing mechanism like electrochemical, catalytic, work-function-based and resistance-based.^[1] However, most of these sensors present limitations that need to be overcome to satisfy the requirements for specific applications. For example, gas chromatography and mass spectroscopy are usual systems for H₂ detection that have an inherent drawback of large hardware size, requiring expensive and constant maintenance.^[1,2] Resistive H₂ sensors based on metal oxide semiconductors generally operate at high temperatures (between 453 K and 723 K) and need a fraction of oxygen in the ambient to detect H₂.^[1,3] For this reason, there is an increasing demand for the development of H₂ sensors that are compact, operate at room temperature, with low cost and improved performance.

Recently, two-dimensional (2D) layered materials have attracted scientific interest due to their properties such as high surface area, low electrical noise, and high electrical conductivity.^[4] With considerable impact on gas sensor applications, 2D materials have their electric conductivity depending on the chemical state of their surface, which drastically changes under adsorption of gas molecules.^[4-6] Such property, for instance, is exploited in graphene researches for detection of distinct gases such as NH₃,^[7] NO₂,^[8] CO₂^[9] and others. In this context, molybdenum disulfide (MoS₂) is one of the most promising transition metal dichalcogenides with great semiconducting properties, including a large intrinsic band gap of 1.8 eV for the monolayer and high current on/off ratios.^[10,11] Few-layer MoS₂ field effect transistors have been particularly successful for applications in nanoelectronics, optoelectronics and gas detection.^[12,13] In fact, MoS₂ transistors have been used to monitor gases such as O₂,^[14] NO,^[15] NH₃,^[16,17] NO₂,^[16-18] and, in general, sensors based on few layers MoS₂ FETs exhibit advantages comparing with bulk sensors such as transparency, cost-effectiveness for massive

This is the authors' version (pre peer-review) of the manuscript: N R. Rezende et al, Advanced Electronic Materials <https://doi.org/10.1002/aelm.201800591> , That has been published in its final form: <https://onlinelibrary.wiley.com/doi/abs/10.1002/aelm.201800591> production and high sensitivity.^[15,16,19] In terms of H₂ sensors by non-functionalized MoS₂ monolayer FETs (MoS₂ FET), the mechanism of detection has not been completely understood yet. Some works propose the H₂ detection mechanism that holds only for more complex structures like MoS₂ nanocomposites films doped with palladium (Pd),^[20] platinum (Pt)^[21] or heterojunctions of MoS₂ films and silicon.^[22] Recently, Agrawal *et al.*^[23] have shown a promising H₂ detection system using edge-oriented vertically aligned MoS₂ flakes in a three-dimensional array without any doping, suggesting that bare MoS₂ has the potential for H₂ detection.

Here, we present a systematic study of the electronic properties of MoS₂ FETs under H₂ gas exposure. The MoS₂ sensors can detect a wide range of H₂ concentration (0.1 % to up to 90 %) as well as operate even at room temperature (300 K). These two characteristics are important for H₂ sensors in practical applications. Our results indicate that the H₂ reaction is independent of the choice of the substrate or metallic contacts. Based on our experimental data and previous density functional theory (DFT) studies, we suggest a model able to explain the electronic response of MoS₂ under interaction with H₂. We believe that H₂ molecules dissociate on the S vacancies (V_S) of MoS₂ transferring charge to MoS₂.^[24-26] This report provides strong evidence that MoS₂ helps the H₂ catalytic reaction with clear implications for hydrogen molecular sensors. Additionally, the understanding of H₂ interaction with MoS₂ is also strategic for industrial processes, such as hydrogen storage and hydrodesulphurization.

2. Results and Discussion

After thermal annealing for 12 hours in ultra-high pure Ar, we investigate the response of the MoS₂ FET supported on SiO₂/Si substrate for molecular hydrogen concentration ($[H_2]$) of 20 % at 473 K. The optical image of the MoS₂ FET is shown in **Figure 1a**. We present the results at such temperature (473K) because of the MoS₂ FET exhibit larger response to the H₂, where faster desorption of H₂ is also obtained, as discussed in detail along this work. Initially, we carried out source-drain current (I_{SD}) vs.

This is the authors' version (pre peer-review) of the manuscript: N R. Rezende et al, Advanced Electronic Materials <https://doi.org/10.1002/aelm.201800591> , That has been published in its final form: <https://onlinelibrary.wiley.com/doi/abs/10.1002/aelm.201800591>

gate voltage (V_G) measurements at fixed source-drain voltage $V_{SD} = 1$ V for distinct H_2 exposure times, as shown in Figure 1b. The cyan (lower) I_{SD} vs. V_G curve represents the standard current (I_{SD}^{INIT}) without the presence of H_2 and the blue (upper) I_{SD} vs. V_G curve corresponds to the saturation after 45 min of H_2 exposure ($I_{SD}^{H_2}$). The saturation criterion used here implies that the transfer curves became constant under H_2 exposure. The characteristics of the I_{SD} vs. V_G curves in Figure 1b represents the typical n-type nature of the MoS_2 channel, which the current increase with the gradual increase in V_G due to the accumulation layer of electrons.^[11] This observation is consistent with previous works, which report that the MoS_2 transistor is predominantly n-type due to the spontaneous doping promoted by the sulfur vacancies.^[27] Furthermore, note that the inset of Figure 1b shows a linear (ohmic) dependence of the I_{SD} vs. V_{SD} without H_2 exposure, excluding the possibility of the Schottky barrier as the dominant transport mechanism.^[11]

In all devices that we measured, the presence of molecular hydrogen causes a leftward shift in the I_{SD} vs. V_G curves, with a simultaneous increase of the I_{SD} current. This modulation of the MoS_2 conductivity indicates a strong response of the MoS_2 FET to H_2 . This leftward shift means that is necessary a more negative V_G turn off the FET, which indicates an increase in the density of MoS_2 carriers after H_2 exposure. Besides, the conductivity change ($\Delta\sigma$) of the MoS_2 channel is expressed by the equation: $\Delta\sigma = e\mu\Delta n$, where e is the electron charge, n is the charge carrier density, and μ is the charge mobility. Thus, a conductivity increase can happen with an increase of charge carrier density or mobility or a combination of both. We discuss what is happening with these properties individually in more detail below.

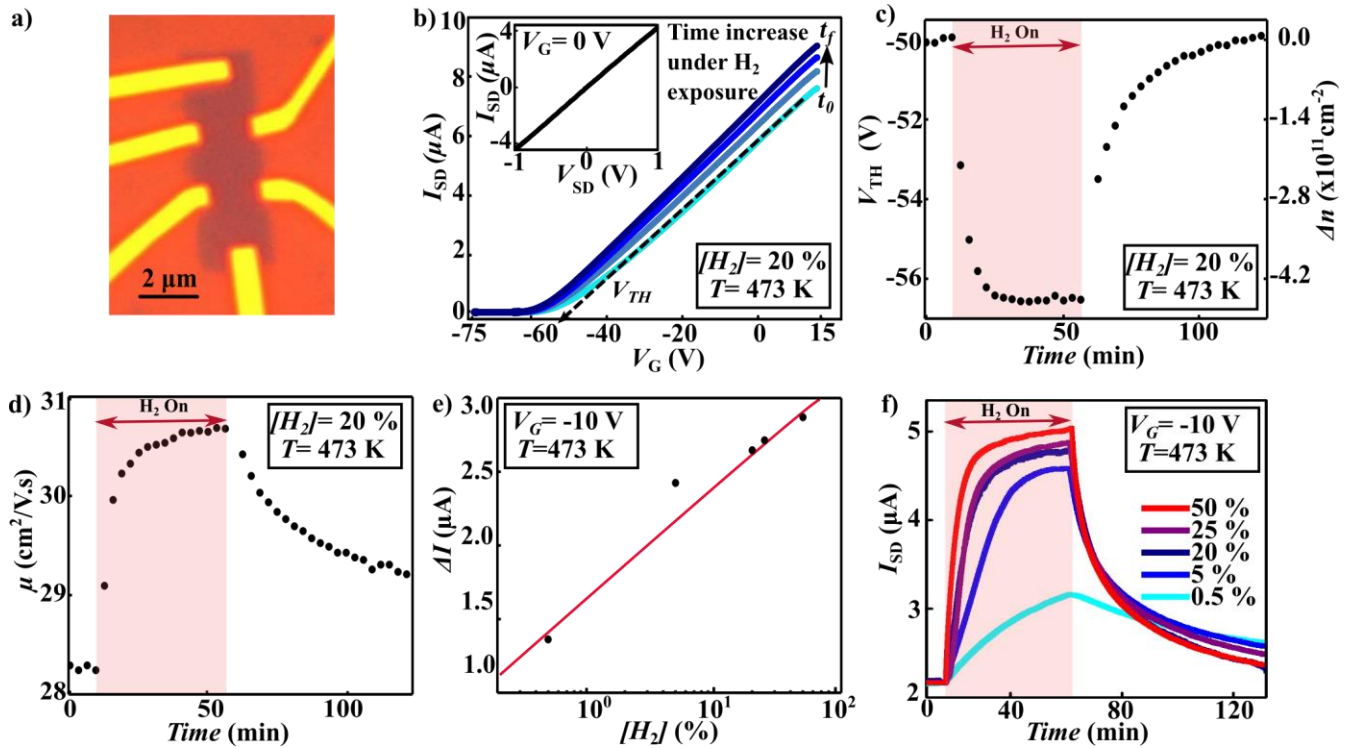


Figure 1. Study of H₂ interaction with MoS₂ FET at 473 K and V_{SD} = 1 V. a) Optical image of a typical MoS₂ FET. In b), c) and d) the data were taken at a fixed hydrogen exposure of [H₂]= 20 %. b) I_{SD} vs. V_G curves of the MoS₂ FET for distinct H₂ exposure times. Inset: I_{SD} vs. V_{SD} curve of the MoS₂ FET for V_G= 0 V, before H₂ exposure. c) The left y-axis shows the threshold voltage (V_{TH}), and the right y-axis axis shows the amount of charge transferred (Δn) to MoS₂ FET as a function of time under H₂ exposure (H₂ ON) and its release in pure Ar. d) FET mobility (μ) as a function of time under H₂ exposure (H₂ ON) and H₂ release. e) Change of drain current ΔI = I_{SD}^{H₂} - I_{SD}^{INIT} as a function of different H₂ concentrations at V_G= -10 V. f) Drain current (I_{SD}) versus time for different H₂ concentrations at V_G = -10 V.

In Figure 1c we plot the values of the threshold voltage (V_{TH}) in the left y-axis as a function of H₂ exposure time. The V_{TH} is obtained by extrapolation of the linear region of the I_{SD} vs. V_G curves presented in Figure 1b. Once the H₂ is introduced into the test chamber, V_{TH} shifts towards negative voltages, indicating that a charge transfer process is taking place due the H₂ adsorption. In this case, a fraction of the H₂ molecules donate electrons to the MoS₂ channel. Next, we shut off the H₂ gas (desorption process), and the threshold voltage returns to its initial value, recovering its condition

This is the authors' version (pre peer-review) of the manuscript: N R. Rezende et al, Advanced Electronic Materials <https://doi.org/10.1002/aelm.201800591> , That has been published in its final form: <https://onlinelibrary.wiley.com/doi/abs/10.1002/aelm.201800591> without H₂ exposure (V_{TH}^{INIT}), indicating the reversibility of the process. The charge transfer process observed is different from what was reported by Agrawal *et al.*^[23] where the H₂ molecules receive electrons from MoS₂. However, our observation is consistent with other MoS₂ film sensors doped with Pd, Pt, and heterojunctions of MoS₂ films and silicon, which propose that hydrogen acts as a reducing agent donating electrons to the MoS₂.^[18,20–22]

The amount of charge per unit of area transferred from hydrogen to the MoS₂ channel (Δn) is shown in the right y-axis of Figure 1c. Δn is evaluated by the following equation $\Delta n = c/e (V_{TH}^{H_2} - V_{TH}^{INIT})$, where $c = \epsilon\epsilon_0/ed$ is the gate capacitance per unit area (12 nF/cm² for 285 nm of SiO₂), e is the electron charge and $V_{TH}^{H_2}$ is the threshold voltage under the H₂ exposure. Interestingly, the negative charge transfer from the H₂ molecules saturates in approximately 4.5×10^{11} cm⁻², suggesting that there is a limited number of active sites of the MoS₂ surface for the H₂ interaction. In addition, we show that the FET mobility (μ) changes during H₂ exposure and desorption in Figure 1d. Noticeably, there is an enhancement of the FET mobility during the adsorption of hydrogen. We believe that such behavior may occurs due to neutralization of charged impurities of the MoS₂ device under H₂ interaction, suggesting a reduction in the charge scattering mechanism. Thus, the conductivity increase in the MoS₂ FET is due to a combination of the increase of charge carrier density and mobility.

Further, we present a study of the MoS₂ FET response concerning molecular hydrogen concentration. Figure 1e shows a linear relationship between the device current ($\Delta I = I_{SD}^{H_2} - I_{SD}^{INIT}$) and $[H_2]$ in a semi-log scale, using a fixed $V_{SD} = 1$ V and $V_G = -10$ V for 0.5, 5, 20, 25 and 50 % of $[H_2]$. Such property can be used as a method to determine the $[H_2]$ inside the test chamber. In Figure 1f we show the I_{SD} vs. *Time* curve. Note that there is a considerably increase in I_{SD} that is strongly related to the hydrogen concentration. Additionally, in the Supplementary Information, we present measurements for another MoS₂ FET in the range of concentrations spanning from 0.1 % up to 90 % of H₂. Hydrogen

This is the authors' version (pre peer-review) of the manuscript: N R. Rezende et al, Advanced Electronic Materials <https://doi.org/10.1002/aelm.201800591> , That has been published in its final form: <https://onlinelibrary.wiley.com/doi/abs/10.1002/aelm.201800591>

concentrations below 0.1 % could not be measured due to limitations of our experimental setup. The mass flow controller used in our experimental setup does not produce reliable values for $[H_2]$ below such amount. However, the device response indicates that the lower bound of the H_2 detection limit is actually lower than our reports. These results demonstrate that the MoS_2 FET is able to detect a large range of H_2 concentrations, as it is required for hydrogen sensors. Usually, the response time (T_{RES}) of a sensor is determined by the time required to reach 90 % of the total conductance change under the gas exposure and the recovery time (T_{REC}) is the time necessary for the current to recover 90 % of its ground state.^[20,22] The minimal T_{RES} is found to be approximately 7 min under 50 % of H_2 (see Figure S1 in Supplementary Information), while the T_{REC} is around 67 min for the same concentration. The response time of a sensor decreases for higher concentrations of hydrogen $[H_2]$. These high recovery and desorption times indicate that the H_2 interaction with the MoS_2 FET is limited by a diffusion reaction. This characteristic will be discussed in detail later.

Next, we show our investigation on the effects of temperature on the hydrogen detection with MoS_2 FETs. In **Figure 2a**, we show the MoS_2 FET sensor response (S) under $[H_2]= 20$ % exposure from 300 K up to 473 K. The sensor response rises up with temperature indicating that the process is thermally activated. Also, we observe a dependency of the device recovering time with temperature. The rate of desorption is slower at 300 K, compared to the rate of desorption at 473 K, meaning that desorption is also a thermally activated process, see Figure 2b. The inset in Figure 2b shows the recovery percentage of intrinsic properties of the MoS_2 FET (Rec) after one hour of H_2 desorption as a function of the temperature, where the red curve is used only as a guide to the eyes. This data supports the reliability of the annealing of MoS_2 FET at 473 K for a couple of hours as an efficient method to speed up the system recovery. Also, thermal annealing is frequently used to restore gas sensors based in 2D materials.^[7,14] The sensor response is generally defined as $S = (I_{SD}^{H_2} - I_{SD}^{INIT}) / I_{SD}^{INIT}$.^[14,15] The sensor

This is the authors' version (pre peer-review) of the manuscript: N R. Rezende et al, Advanced Electronic Materials <https://doi.org/10.1002/aelm.201800591> , That has been published in its final form: <https://onlinelibrary.wiley.com/doi/abs/10.1002/aelm.201800591> response as a function of the temperature is obtained by $I_{SD} \times V_G$ curves measured with fixed $V_G = -10$ V. Nevertheless, the values of S retrieved in this configuration show the same behavior for other gate values.

For a better understanding of the reversibility of the process at 473 K, we carried out experiments with longer H₂ exposure times (see Figure S2 in Supplementary Information). We observe that for 473 K, the MoS₂ FET operates reproducibly, showing the same response repeated times. The initial conditions are fully recovered after a couple of hours without H₂ interaction in all cases. Such full recovery indicates that neither permanent bonds nor defect creation occur between H₂ molecules and MoS₂. Indeed, we confirmed this assumption by performing Raman spectroscopy of the monolayer before and after H₂ exposure (Figure S3 in Supplementary Information). We do not observe any indication of structural changes or irreversible chemical bonding after exposing the devices to H₂, which should be detected by changes in the Raman spectrum.^[28] More precisely, no change of the Raman peaks E_{2g}^1 and A_{1g} of the MoS₂ is observed.

Subsequently, we investigate the dependence of the sensor response with the applied gate voltage. Previous works showed that the response of sensors based in MoS₂ for O₂,^[14] NO₂ and NH₃^[16] detection is improved in a given range of gate voltages. We also observed this behavior for hydrogen sensor response in our devices, as shown in Figure 2c. S becomes remarkably higher for negative gates. The inset of Figure 2c shows that the V_{TH} for this device is approximate -16 V, when the voltage approaches this value, S increases rapidly. This means that the introduction of H₂ in the off-state of the transistor makes the current change more significantly than in the condition with the MOS₂ FET initially in on-state

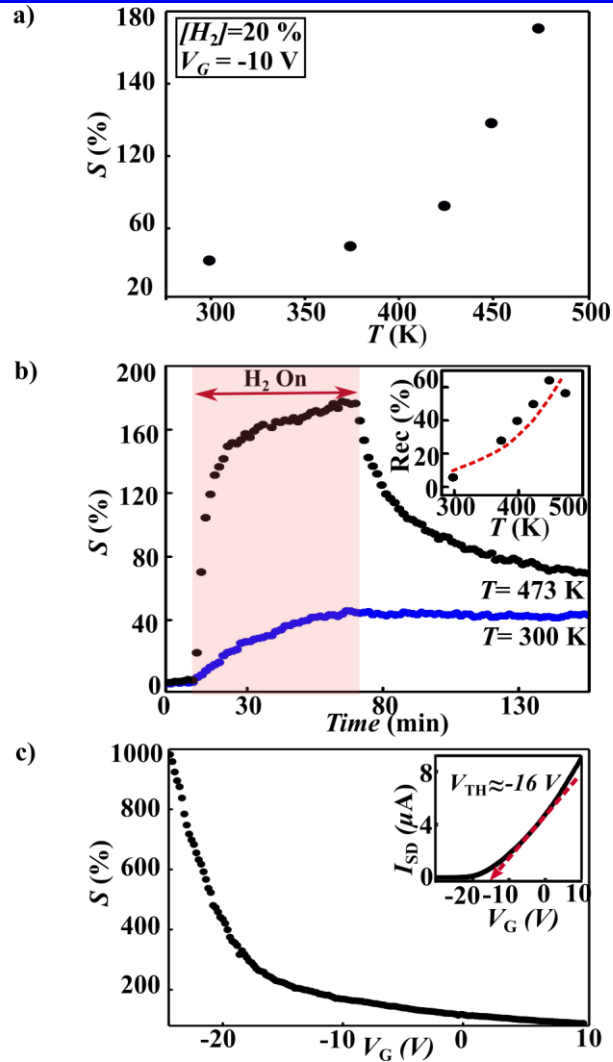


Figure 2. Sensing performance of MoS₂ FET for a fixed H₂ concentration of $[H_2]= 20\%$ and $V_{SD}= 1$ V. In a) and b) the data were taken at a fixed $V_G= -10$ V. a) Sensor response (S) of MoS₂ FET as a function of temperature: from 300 K up to 473 K. b) Comparison of sensor response as function of time under the H₂ exposure (H₂ ON) at 300 K (black curve) and 473 K (blue curve). Inset: Recovery (Rec) percentage after one hour of H₂ desorption as a function of the temperature. c) Sensor response as a function of gate voltage at 473 K. Inset: I_{SD} vs. V_G curve of the MoS₂ transistor.

Now, we show our investigation trying to elucidate how MoS₂ FETs detect molecular hydrogen. In this context, we carry out experiments specifically designed to clarify: (1) If there is the detection of hydrogen at the MoS₂/metal interface. For example, there are H₂ sensors based on the modulation of the electrostatic properties of heterojunctions between the metal contact/2D materials and sensors based on the Schottky barrier effect.^[1,16,29–31] (2) If the detection of H₂ depends on the underlying substrate.

This is the authors' version (pre peer-review) of the manuscript: N R. Rezende et al, Advanced Electronic Materials <https://doi.org/10.1002/aelm.201800591> , That has been published in its final form: <https://onlinelibrary.wiley.com/doi/abs/10.1002/aelm.201800591>

Previous reports have shown that oxygen gas could interact with graphene devices on SiO₂/Si substrates via the incorporation of O₂ molecules between the substrate and the graphene causing a change in its FET mobility.^[32] (3) And, finally, if the H₂ detection is mainly related to intrinsic properties of MoS₂. In this case, the mechanism is driven by dissociative adsorption of hydrogen at sulfur vacancies of MoS₂. This possibility could explain there is a charge transferring to MoS₂ under interaction with H₂. Below we discuss each of these points separately.

To check if there is the detection of hydrogen at the interface between MoS₂ and the contact metal, or if the contact resistance changes under interaction with H₂, we perform measurements in two and four-probe (Hall bar) configurations. It is reasonable to assume that the total change in conductance (ΔG) of MoS₂ FET due to H₂ adsorption is represented by $\Delta G = \Delta G_{\text{Channel}} + \Delta G_{\text{Contacts}}$, where $\Delta G_{\text{Channel}}$ is directly proportional to the carrier concentration injected in the channel and $\Delta G_{\text{Contacts}}$ is inversely proportional to the contact resistance change. Besides, it is known that the four-probe configuration eliminates the influence of contact resistance; in this case, we can detect only the change in conductance due to the charge transfer to the MoS₂ channel ($\Delta G = \Delta G_{\text{Channel}}$).^[14,31] Therefore, if H₂ sensing is dominated by the contact resistance, i.e., H₂ molecules change the Schottky barrier height via modulation of the metal work function, we would not expect to measure a significant hydrogen response in a four-probe configuration. **Figure 3a** shows the sensor response as a function of the H₂ exposure measured in two and four-probe configurations, represented by the black and green curve, respectively (more details are provided in the Supplementary information). Since S exhibits the same magnitude for both configurations, we infer that the sensing mechanism does not depend on the electrostatic configuration at the MoS₂/metal contact interface. This is also an expected result since our Au/MoS₂ contacts have ohmic behavior as depicted in the inset of Figure 1(b).

This is the authors' version (pre peer-review) of the manuscript: N R. Rezende et al, Advanced Electronic Materials <https://doi.org/10.1002/aelm.201800591> , That has been published in its final form: <https://onlinelibrary.wiley.com/doi/abs/10.1002/aelm.201800591>

Next, we consider the influence of the underline substrate on the H₂ detection by MoS₂ FETs.

Trying to understand the role of the substrate in the hydrogen response, we produced a device with MoS₂ supported on h-BN. The h-BN has an inert and flat surface that enables the creation of only a few charge impurities, in contrast to the abundance of trap states that are present in the interface with SiO₂/Si substrates.^[33,34] We suspected that H₂ could interact with substrate defects and dangling bonds causing changes in MoS₂ electronic mobility, such as those shown in Figure 1d. In this case, the total change in the MoS₂ conductance due to H₂ adsorption would be represented by $\Delta G = \Delta G_{\text{Channel}} + \Delta G_{\text{SiO}_2}$, where ΔG_{SiO_2} represents the increase in the conductance due to the interaction or screening of defects of the substrate after the hydrogen passivation. In Figure 3b we show the comparison of the sensor response of the SiO₂/Si (black curve) and h-BN substrate (green curve) as a function of the threshold voltage difference ($V_G - V_{\text{TH}}$). Such normalization (plotted in the x-axis) is adopted because the devices have different V_{TH} and, as previously shown, S depends on the gate voltage. These results reveal that the sensor response is nearly the same for both substrates providing strong evidence that the sensing mechanism does not involve possible interactions between H₂ molecules with the underlying substrate. A more complete overview of MoS₂ FET supported on h-BN interaction with H₂ is found in the Supplementary Information (Figure S4). All fabricated devices present the same sensor response as a function of temperature and H₂ concentration as the MoS₂ supported on SiO₂/Si.

Based on the analysis presented above, we can assert that the H₂ sensing mechanism occurs in the MoS₂ main channel. Therefore, at this point, we need to elucidate how the interaction of H₂ with the MoS₂ results in the conductance change of the MoS₂ in a reversible process. Some hypothesis can be drawn to explain the conductivity enhancement based in previously reported studies.^[35,36] The main mechanism proposed here is the dissociative adsorption of hydrogen facilitated by the catalytic

This is the authors' version (pre peer-review) of the manuscript: N R. Rezende et al, Advanced Electronic Materials <https://doi.org/10.1002/aelm.201800591> , That has been published in its final form: <https://onlinelibrary.wiley.com/doi/abs/10.1002/aelm.201800591>

properties of MoS₂, as illustrated in Figure 4. The ΔG , in this case, is driven by the charge transfer mechanism from H₂ molecules to the MoS₂ channel, represented by the following H₂ reaction: $H_2 \xrightarrow{MoS_2} 2H^+ + 2e^-$. In this scenario, absorbed H atoms donate electrons to the conduction band of MoS₂, producing the sensor response. Theoretical and experimental works report that the existence of V_S increase the catalytic activity of MoS₂.^[37,38] These references show that the hydrogen evolution is effectively improved due to the creation of V_S in the monolayer MoS₂.^[37,38]

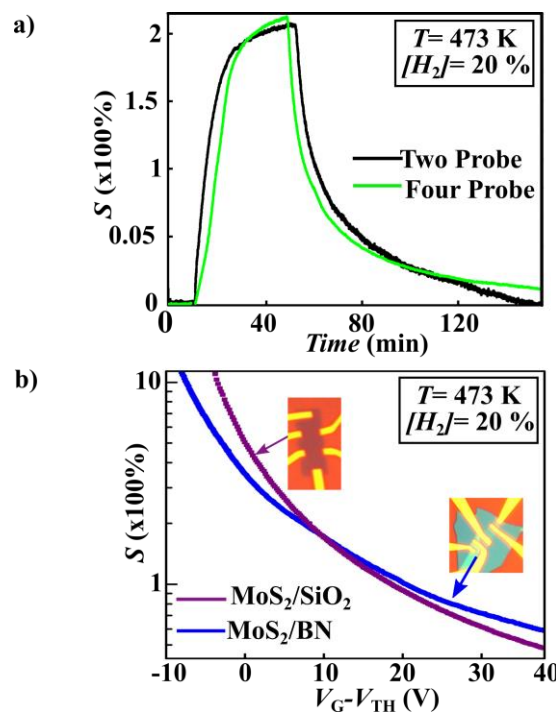


Figure 3. Influence of MoS₂ FET interfaces on the H₂ sensing mechanism. Sensing performance of MoS₂ monolayer transistor in a) and b) study for the H₂ concentration of $[H_2] = 20\%$ and 473 K. a) Comparison of MoS₂ FET sensor response in two-probe and four-probe (Hall bar) measurements. b) Sensor response versus threshold normalized voltage ($V_G - V_{TH}$) for MoS₂ FETs supported on SiO₂/Si and the h-BN substrate.

Now we discuss in details the H₂ dissociative adsorption regarding absence and presence of sulfur defective sites in the MoS₂ surface. If a perfect MoS₂ monolayer is considered, H atoms can bond to the sulfur atoms or molybdenum atoms after H₂ dissociation. Theoretical works show that H atoms prefer to bond to sulfur atoms, presenting relatively lower energy concerning Mo atoms. The adsorbed H atoms affect the electronic property of MoS₂, promoting a metallization of the surface due to the electron donation.^[24,36,39] Yakovkin *et al.*^[39] have investigated the relative instability of this bond, and

This is the authors' version (pre peer-review) of the manuscript: N R. Rezende et al, *Advanced Electronic Materials* <https://doi.org/10.1002/aelm.201800591>, That has been published in its final form: <https://onlinelibrary.wiley.com/doi/abs/10.1002/aelm.201800591> suggested that some H atoms can overcome the potential barrier for desorption and form H₂ molecules at high temperature.

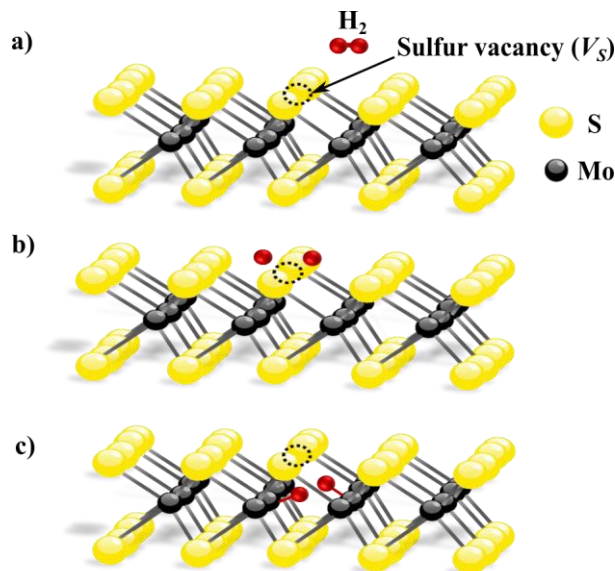


Figure 4: Representation of the dissociative adsorption of H₂ on the sulfur vacancy (V_S). a) The hydrogen molecule approaches to the MoS₂ surface; b) The dissociation of H₂ is induced by the presence of a sulfur vacancy; c) Adsorption of H atoms in defective sites, forming H-Mo bonds.

On the other hand, DFT studies indicate that molecular hydrogen adsorption is more favorable in the MoS₂ surface if sulfur defective sites are present (**Figure 4a**), exhibiting a more effective energetic scenario than in a perfectly stoichiometric MoS₂ surface,^[24,25] in accordance with other works that study the catalytic properties of MoS₂.^[37,38] In this case, after H₂ dissociation (Figure 4b), H atoms bond to unsaturated molybdenum atoms,^[25,26] as illustrated in Figure 4c. Considering the arguments presented above, and the finding that V_S is generated in the mechanical exfoliation carried out for the preparation of MoS₂ monolayers,^[40] we suggest that the electron donation from the hydrogen molecules probably originates from the dissociative adsorption of H₂ due the presence of V_S.

To investigate the role of V_S in hydrogen adsorption, we cover the MoS₂ surface with aluminum oxide (Al₂O₃) layers using atomic layer deposition (ALD) and monitor the response of such hybrid MoS₂/Al₂O₃ FET to H₂. Different coverages of Al₂O₃ are directly deposited on the top of the MoS₂ device at 373 K, using TMA (Trimethyl Aluminum) and H₂O precursors. Previous works showed that

This is the authors' version (pre peer-review) of the manuscript: N R. Rezende et al, Advanced Electronic Materials <https://doi.org/10.1002/aelm.201800591> , That has been published in its final form: <https://onlinelibrary.wiley.com/doi/abs/10.1002/aelm.201800591> the Al₂O₃ grows preferentially on terrace edges and localized defects, where the covalent lattice is discontinued breaking the surface periodicity.^[41,42] Therefore, the Al₂O₃ clusters bind the intrinsic defects, including the V_S in the MoS₂ monolayer. Based on the assumption that the sensor response depends on the dissociative adsorption of hydrogen in the V_S, we expect to see a lower sensitivity to H₂ molecules after the Al₂O₃ deposition. More details about the ALD steps to produce the MoS₂/Al₂O₃ FET and the AFM image before and after the Al₂O₃ grown are available in the Supplementary Information.

In **Figure 5a** we show the sensor response of a MoS₂ FET submitted to 5 growth pulses of Al₂O₃ and the bare MoS₂ device. This number of cycles was adopted to avoid the formation of an Al₂O₃ film on the MoS₂ device, solely promoting the passivation of V_S. The dotted curves represent the standard current, and the solid curves represent the current after 60 min of H₂ exposure at 473 K and [H₂] = 20 %. According to these transfer curves, we observe that the current of MoS₂/Al₂O₃ FET (red curves), increases compared to the initial values for the bare MoS₂ FET (black curves). The FET mobility also increases from approximately 34 to 52 cm²/V.s. This behavior is consistent with the dielectric screening effects from the Al₂O₃ overlayer observed in previous studies reported in the literature.^[43]

We should point out that we continue to observe H₂ interaction after the Al₂O₃ growth. Most importantly, we notice a reduction in the charge transfer from hydrogen to the MoS₂ channel, indicating a decrease in the number of active sites of the MoS₂ surface for the H₂ interaction. The charge transfer for the bare MoS₂ FET is approximately $n \sim 7.4 \times 10^{11} \text{ cm}^{-2} \text{V}^{-1}$ while for the MoS₂/Al₂O₃ FET is $n \sim 3 \times 10^{10} \text{ cm}^{-2} \text{V}^{-1}$. We estimate the charge transfer by the V_{TH} shift obtained by the extrapolation of the linear region between -17 V to -20 V, for the I_{SD} vs. V_G curves presented in Figure 5a. This behavior also occurs for devices in which a large amount of Al₂O₃ pulses is used.

This is the authors' version (pre peer-review) of the manuscript: N R. Rezende et al, Advanced Electronic Materials <https://doi.org/10.1002/aelm.201800591> , That has been published in its final form: <https://onlinelibrary.wiley.com/doi/abs/10.1002/aelm.201800591>

To demonstrate the reduction of the MoS₂ reactivity to H₂ after the Al₂O₃ growth, we present in Figure 5b the current gain (I_{H_2}/I_{Ar}) as a function of the threshold voltage difference ($V_G - V_{TH}$), this normalization again was adopted because V_{TH} changes drastically after the oxide growth. The current gain is lower for the MoS₂/Al₂O₃ hybrid device represented by the red curve in Figure 5b than the bare MoS₂ device (black curve). Besides, I_{H_2}/I_{Ar} for MoS₂/Al₂O₃ FET is close to 1, indicating a small increase in current compared to its initial value without H₂ exposure. Additionally, the inset in Figure 5b shows the S decrease after the Al₂O₃ growth. Such reductions in the current gain and sensor response demonstrate partial passivation of the reactive sites to hydrogen dissociative adsorption in the monolayer, evidencing that the V_s play an important role in the H₂ interaction with the MoS₂. A similar decrease of the sensitivity of the H₂ detection system using edge-oriented vertically aligned MoS₂ flakes was observed after the passivation of the edges using ZnO films.^[23]

Nonetheless, MoS₂ interaction with hydrogen continues to occur even after Al₂O₃ growth. Since H₂ is a small molecule and can reach both sides of the MoS₂ sheet (top and bottom side), one cannot disregard that hydrogen also interacts with the bottom side of the MoS₂ layer, producing the hydrogen response. This observation is also consistent with the high response and desorption times obtained for the MoS₂ FET sensors. The top side and bottom side of the monolayer are not equally accessible to H₂ molecules. Thus, two different mechanisms of interaction occur (see Fig S7 in SI). We believe that the fast increase (decrease, in case of the desorption process) of the current is explained by the reaction of H₂ with the top of the monolayer, while the longer response time for current saturation (or recovery) is explained by the diffusion of H₂ molecules in between MoS₂ and the substrate. Furthermore, the even higher H₂ desorption time in comparison with the H₂ adsorption time is related with the state of the “trapped” H₂ molecules in between the MoS₂ and the substrate having more difficult to be desorbed. Interestingly, the response and recovering time in the MoS₂/Al₂O₃ FET is longer than the bare MoS₂, as

This is the authors' version (pre peer-review) of the manuscript: N R. Rezende et al, Advanced Electronic Materials <https://doi.org/10.1002/aelm.201800591> , That has been published in its final form: <https://onlinelibrary.wiley.com/doi/abs/10.1002/aelm.201800591> shown in the red curve of Figure 5c. This result is consistent with mostly the diffusion of hydrogen between the MoS₂ sheet and the SiO₂/Si substrate, and the attenuation of the fast adsorption mechanism at the top of the monolayer.

Finally, our work shows that the modulation of the conductivity of the MoS₂ monolayer channel dominates the H₂ sensing process. We propose that such modulation originates from a charge transfer process associated with the dissociative H₂ adsorption. Such adsorption is a thermally activated process (as shown in Figure 2a) that is facilitated by the presence of V_S in the monolayer.^[24,25] The effectiveness of V_S to induce the charge transfer reaction implies that there is a limited number of sites for the reaction to occur, corroborating our results of charge-transfer saturation, as shown in Figure 1c. After aluminum oxide passivation of the top side of the monolayer, we yet detect hydrogen, but the sensor response decreases. This result is a clear indication that the V_S plays an important role in the H₂ interaction with the MoS₂ and corroborates the idea that the gas molecule interacts with both sides of the MoS₂ sheet. Therefore, we believe that the sensor performance can be enhanced by the increase of V_S on the MoS₂ surface. For instance, Donarelli *et al.* ^[44] proposed the creation of sulfur vacancies of MoS₂ by thermal annealing in an ultra-high vacuum. An increase in the device mobility due to the H₂ presence is also observed that can be attributed to the screening of MoS₂ defective sites due to the hydrogen molecules adsorption. Besides, we believe that the existence of V_S can contribute to the instability of the hydrogen adsorption, corroborated by the reversibility behavior of the reaction.

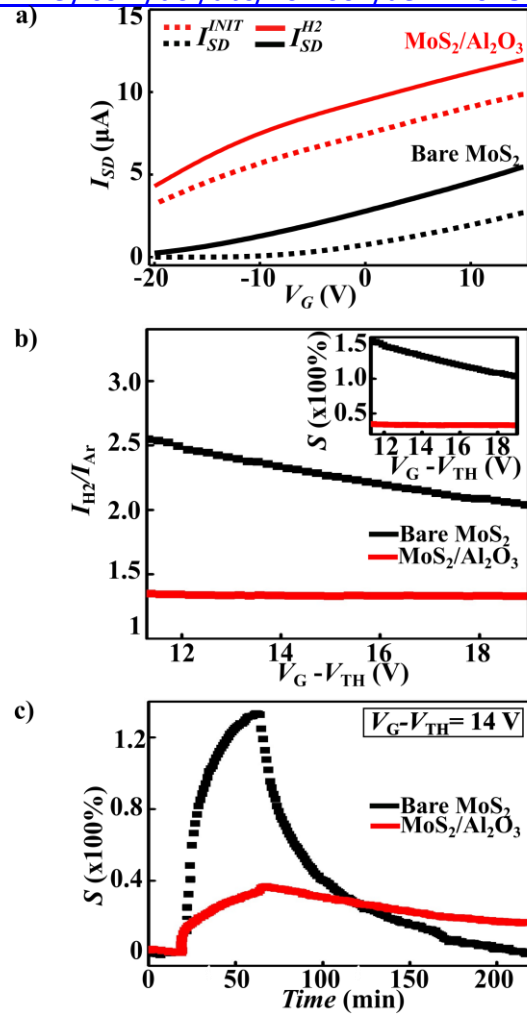


Figure 5. Comparison of sensing performance of MoS₂ monolayer and MoS₂/Al₂O₃ transistors are shown in a), b) and c), all studied for a fixed [H₂] = 20 %, V_{SD}=1 V and 473 K. a) I_{SD} vs. V_G curves of the bare MoS₂ (black color), and MoS₂ with 5 cycles of Al₂O₃ growth (red color) before (dotted line) and after (solid lines) the H₂ exposure. b) Current gain (I_{H2}/I_{Ar}) as a function of the threshold voltage difference (V_G-V_{TH}) for bare MoS₂ and MoS₂/Al₂O₃ FETs. Inset: Sensor response as a function of the threshold voltage difference. c) Sensor response as a function of time during the H₂ exposure, in fixed threshold voltage difference (V_G-V_{TH}) = 14 V.

3. Conclusion

We investigated the H₂ interaction with monolayer MoS₂ devices. Both the adsorption and desorption gas processes are strongly dependent on the temperature, and the sensing is independent of the choice of the substrate or metallic contacts. Our experimental data suggest that the charge transfer process from H₂ to the MoS₂ channel dominates the sensing process. We propose that the charge

This is the authors' version (pre peer-review) of the manuscript: N R. Rezende et al, Advanced Electronic Materials <https://doi.org/10.1002/aelm.201800591> , That has been published in its final form: <https://onlinelibrary.wiley.com/doi/abs/10.1002/aelm.201800591> transfer originates from the dissociative H₂ adsorption, which is facilitated by the presence of Vs in the MoS₂. We also discussed evidence that the molecular hydrogen can interact on both sides of the MoS₂ sheet (top side and bottom side) based on our measurements of MoS₂/Al₂O₃ heterojunctions. Finally, we demonstrated that the MoS₂ device is a promising candidate for the development of molecular hydrogen sensors. The MoS₂ sensor responds to a wide range of hydrogen concentrations, operates at relatively low temperatures and do not require the presence of catalytic metals dopants (Pd, Pt), and can be fully recovered. Our findings also provide insights for future applications in catalytic processes making use of monolayer MoS₂ FETs.

4. Experimental Section

Device Fabrication: To investigate the molecular hydrogen interaction with MoS₂ FET, we produce several devices supported on two different substrates: Si covered with 285 nm of SiO₂ (SiO₂/Si) and hexagonal boron nitride (h-BN). To obtain the monolayer MoS₂, we used mechanical exfoliation with scotch tape technique.^[45] To prepare the MoS₂ FET supported on h-BN, firstly, the mechanically exfoliated h-BN flakes are directly transferred from the tape to the SiO₂/Si substrate. After that, we use the dry viscoelastic stamping technique to transfer the MoS₂ in the top of h-BN/SiO₂/Si flakes.^[46] The metallic contacts of both device types are fabricated employing standard electron beam lithography and thermal metal deposition of Au (50nm). Finally, we use a second lithography step and SF₆ plasma etching to define the MoS₂ device geometry.

In situ Electrical Measurements: After fabrication, the MoS₂ FET is fixed on a chip holder and transferred into a chamber connected to an electrical measurement system. We use a heater to control the temperature inside the chamber in the range of 300 K–473 K. The H₂ flow is determined by a mass flow controller and dilution with ultra-high pure argon (Ar) is used to obtain different H₂

This is the authors' version (pre peer-review) of the manuscript: N R. Rezende et al, Advanced Electronic Materials <https://doi.org/10.1002/aelm.201800591> , That has been published in its final form: <https://onlinelibrary.wiley.com/doi/abs/10.1002/aelm.201800591> concentrations. More details of the gas sensing system can be found in our previous work.^[7] Before carrying out electrical measurements under hydrogen exposure, we perform an annealing procedure in all devices presented in this work in Ar atmosphere at 473 K for 12 hours. This thermal treatment is known to promote the removal of contaminating gases and humidity.^[7,31,32] We use the external DC source of a lock-in amplifier (SR830) to provide a source-drain voltage (V_{SD}) and a Keithley K2400 source to provide a DC gate voltage (V_G). The current between the source and drain (I_{SD}) is collected by a pre-amplifier and measured by a Keithley 2000 Digital Multimeter.

Supporting Information

Supporting Information is available from the Wiley Online Library or from the author.

Acknowledgments:

This work was supported by CAPES, Fapemig (Rede 2D), CNPq and INCT/Nanomaterials de Carbono. The authors are thankful Lab Nano at UFMG for allowing the use of atomic force microscopy and CT Nano at UFMG for the Raman measurements. We acknowledge S. L. M. Ramos for the Raman measurements and E. S. N. Gomes for helping with the Raman analyses. We also acknowledge M. S. C, Mazzoni for helping with theoretical discussions about phenomenology. K.W. and T.T. acknowledge support from the Elemental Strategy Initiative conducted by the MEXT, Japan and JSPS KAKENHI Grant Numbers JP15K21722.

This is the authors' version (pre peer-review) of the manuscript: N R. Rezende et al, Advanced Electronic Materials <https://doi.org/10.1002/aelm.201800591> , That has been published in its final form: <https://onlinelibrary.wiley.com/doi/abs/10.1002/aelm.201800591>

References

- [1] T. Hübert, L. Boon-brett, G. Black, U. Banach, *Sensors Actuators B. Chem.* **2011**, *157*, 329.
- [2] P. Soundarrajan, F. Schweighardt, in *Hydrog. Fuel Prod. Transp. Storage*, CRC Press, **2008**, pp. 495–533.
- [3] S. Öztürk, N. Kılınç, İ. Torun, A. Kösemen, Y. Şahin, Z. Z. Öztürk, *Int. J. Hydrogen Energy* **2014**, *39*, 5194.
- [4] S. S. Varghese, S. S. Varghese, S. Swaminathan, K. Singh, V. Mittal, *Electronics* **2015**, *4*, 651.
- [5] W. Yang, L. Gan, H. Li, T. Zhai, *Inorg. Chem. Front.* **2016**, *3*, 433.
- [6] S. Yang, C. Jiang, S. Wei, *Appl. Phys. Rev.* **2017**, *4*, 021304.
- [7] A. R. Cadore, E. Mania, A. B. Alencar, N. P. Rezende, S. de Oliveira, K. Watanabe, T. Taniguchi, H. Chacham, L. C. Campos, R. G. Lacerda, *Sensors Actuators B Chem.* **2018**, *266*, 438.
- [8] R. Pearce, T. Iakimov, M. Andersson, L. Hultman, A. L. Spetz, R. Yakimova, *Sensors Actuators B. Chem.* **2011**, *155*, 451.
- [9] H. Joong, D. Han, J. Ho, Z. Zhou, *Sensors Actuators B. Chem.* **2011**, *157*, 310.
- [10] K. F. Mak, C. Lee, J. Hone, J. Shan, T. F. Heinz, *Phys. Rev. Lett.* **2010**, *105*, 136805.
- [11] B. Radisavljevic, A. Radenovic, J. Brivio, V. Giacometti, A. Kis, *Nat. Nanotechnol.* **2011**, *6*, 147.
- [12] R. Ganatra, Q. Zhang, *ACS Nano* **2014**, *8*, 4074.
- [13] X. Tong, E. Ashalley, F. Lin, H. Li, Z. M. Wang, *Nano-Micro Lett.* **2015**, *7*, 203.
- [14] Y. Tong, Z. H. Lin, J. T. L. Thong, D. S. H. Chan, C. X. Zhu, *Appl. Phys. Lett.* **2015**, *107*, 5.
- [15] H. H. Li, Z. Yin, Q. He, H. H. Li, X. Huang, G. Lu, D. W. H. Fam, A. I. Y. Tok, Q. Zhang, H. Zhang, *Small* **2012**, *8*, 63.
- [16] B. Liu, L. Chen, G. Liu, A. N. Abbas, M. Fathi, C. Zhou, *ACS Nano* **2014**, *8*, 5304.
- [17] D. J. Late, Y. K. Huang, B. Liu, J. Acharya, S. N. Shirodkar, J. Luo, A. Yan, D. Charles, U. V. Waghmare, V. P. Dravid, C. N. R. Rao, *ACS Nano* **2013**, *7*, 4879.
- [18] M. Donarelli, S. Prezioso, F. Perrozzi, F. Bisti, M. Nardone, L. Giancaterini, C. Cantalini, L. Ottaviano, *Sensors Actuators B Chem.* **2015**, *207*, 602.
- [19] I. Song, C. Park, H. C. Choi, *RSC Adv.* **2015**, *5*, 7495.
- [20] C. Kuru, C. Choi, A. Kargar, D. Choi, Y. J. Kim, C. H. Liu, S. Yavuz, S. Jin, *Adv. Sci.* **2015**, *2*, 1500004.
- [21] B. K. Miremadi, R. C. Singh, S. R. Morrison, K. Colbow, *Appl. Phys. A* **1996**, *63*, 271.
- [22] Y. Liu, L. Hao, W. Gao, Z. Wu, Y. Lin, G. Li, W. Guo, L. Yu, H. Zeng, J. Zhu, W. Zhang, *Sensors Actuators, B Chem.* **2015**, *211*, 537.
- [23] A. V. Agrawal, R. Kumar, S. Venkatesan, A. Zakhidov, Z. Zhu, J. Bao, M. Kumar, M. Kumar, *Appl. Phys. Lett.* **2017**, *111*, 093102.
- [24] E. W. Keong Koh, C. H. Chiu, Y. K. Lim, Y. W. Zhang, H. Pan, *Int. J. Hydrogen Energy* **2012**, *37*, 14323.
- [25] D. C. Sorescu, D. S. Sholl, A. V Cugini, *J. Phys. Chem. B* **2004**, *108*, 239.
- [26] S. W. Han, G. B. Cha, Y. Park, S. C. Hong, *Sci. Rep.* **2017**, *7*, 7152.
- [27] D. Liu, Y. Guo, L. Fang, J. Robertson, *Appl. Phys. Lett.* **2013**, *103*, 183113.
- [28] B. H. Kim, M. Park, M. Lee, S. J. Baek, H. Y. Jeong, M. Choi, S. J. Chang, W. G. Hong, T. K. Kim, H. R. Moon, Y. W. Park, N. Park, Y. Jun, *RSC Adv.* **2013**, *3*, 18424.
- [29] K. Skucha, Z. Fan, K. Jeon, A. Javey, B. Boser, *Sensors Actuators, B Chem.* **2010**, *145*, 232.
- [30] K. Zdansky, *Nanoscale Res. Lett.* **2011**, *6*, 1.

This is the authors' version (pre peer-review) of the manuscript: N R. Rezende et al, Advanced Electronic Materials <https://doi.org/10.1002/aelm.201800591> , That has been published in its final form: <https://onlinelibrary.wiley.com/doi/abs/10.1002/aelm.201800591>

- [31] A. R. Cadore, E. Mania, E. A. De Morais, K. Watanabe, T. Taniguchi, R. G. Lacerda, L. C. Campos, *Appl. Phys. Lett.* **2016**, *109*, 033109.
- [32] I. Silvestre, E. A. De Morais, A. O. Melo, L. C. Campos, A. M. B. Goncalves, A. R. Cadore, A. S. Ferlauto, H. Chacham, M. S. C. C. Mazzoni, R. G. Lacerda, *ACS Nano* **2013**, *7*, 6597.
- [33] M. K. Joo, B. H. Moon, H. Ji, G. H. Han, H. Kim, G. Lee, S. C. Lim, D. Suh, Y. H. Lee, *Nano Lett.* **2016**, *16*, 6383.
- [34] M. Y. Chan, K. Komatsu, S.-L. Li, Y. Xu, P. Darmawan, H. Kuramochi, S. Nakaharai, A. Aparecido-Ferreira, K. Watanabe, T. Taniguchi, K. Tsukagoshi, *Nanoscale* **2013**, *5*, 9572.
- [35] M. Calandra, *Phys. Rev. B - Condens. Matter Mater. Phys.* **2013**, *88*, 245428.
- [36] S. W. Han, W. S. Yun, J. D. Lee, Y. H. Hwang, J. Baik, H. J. Shin, W. G. Lee, Y. S. Park, K. S. Kim, *Phys. Rev. B - Condens. Matter Mater. Phys.* **2015**, *92*, 241303.
- [37] G. Ye, Y. Gong, J. Lin, B. Li, Y. He, S. T. Pantelides, W. Zhou, R. Vajtai, P. M. Ajayan, *Nano Lett.* **2016**, *16*, 1097.
- [38] H. Li, C. Tsai, A. L. Koh, L. Cai, A. W. Contryman, A. H. Fragapane, J. Zhao, H. S. Han, H. C. Manoharan, F. Abild-Pedersen, J. K. Nørskov, X. Zheng, *Nat. Mater.* **2015**, *15*, 48.
- [39] I. N. Yakovkin, N. V. Petrova, *Chem. Phys.* **2014**, *434*, 20.
- [40] J. Hong, Z. Hu, M. Probert, K. Li, D. Lv, X. Yang, L. Gu, N. Mao, Q. Feng, L. Xie, J. Zhang, D. Wu, Z. Zhang, C. Jin, W. Ji, X. Zhang, J. Yuan, Z. Zhang, *Nat. Commun.* **2015**, *1*, 011002.
- [41] M. De Pauli, M. J. S. Matos, P. F. Siles, M. C. Prado, B. R. A. Neves, S. O. Ferreira, M. S. C. Mazzoni, A. Malachias, *J. Phys. Chem. B* **2014**, *118*, 9792.
- [42] S. Park, S. Y. Kim, Y. Choi, M. Kim, H. Shin, J. Kim, W. Choi, *ACS Appl. Mater. Interfaces* **2016**, *8*, 11189.
- [43] S.-W. Min, H. S. Lee, H. J. Choi, M. K. Park, T. Nam, H. Kim, S. Ryu, S. Im, *Nanoscale* **2013**, *5*, 548.
- [44] M. Donarelli, F. Bisti, F. Perrozzi, L. Ottaviano, *Chem. Phys. Lett.* **2013**, *588*, 198.
- [45] K. S. Novoselov, D. Jiang, F. Schedin, T. J. Booth, V. V. Khotkevich, S. V. Morozov, A. K. Geim, T. M. Rice, *Proc. Natl. Acad. Sci.* **2005**, *102*, 10451.
- [46] A. Castellanos-Gomez, M. Buscema, R. Molenaar, V. Singh, L. Janssen, H. S. J. Van Der Zant, G. A. Steele, *2D Mater.* **2014**, *1*, DOI 10.1088/2053-1583/1/1/011002.

Supporting Information

Probing the Electronic Properties of Monolayer MoS₂ via Interaction with Molecular Hydrogen

*Natália P. Rezende, Alisson R. Cadore, Andreij C. Gadelha, Cíntia L. Pereira, Vinicius Ornelas, Kenji Watanabe, Takashi Taniguchi, André S. Ferlauto, Ângelo Malachias, Leonardo C. Campos, and Rodrigo G. Lacerda**

1. Evaluation of response time of MoS₂ FETs at 473 K for distinct [H₂]

Figure S1 shows the response time of a MoS₂ FET subjected to distinct H₂ concentrations at 473 K. The saturation current was estimated by the exponential fit of the $I_{SD} \times Time$ curves shown in Figure 1e of the main text. The response time of a sensor decreases with the increase in [H₂]. This phenomenon may be related to the T_{RES} definition, since an increase in the number of hydrogen molecules in the MoS₂ surface leads to a faster current saturation.

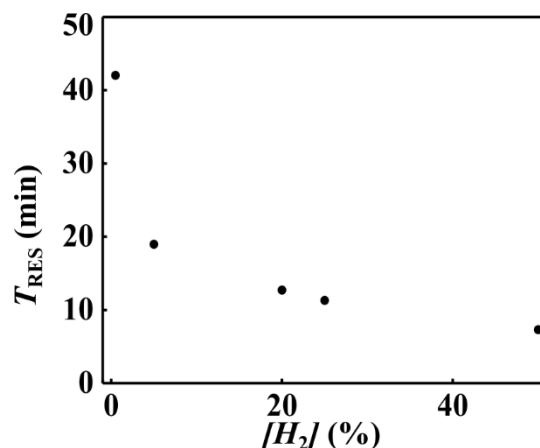


Figure S1: Response time of MoS₂ FETs for different H₂ concentrations of [H₂] at 473 K.

This is the authors' version (pre peer-review) of the manuscript: N R. Rezende et al, Advanced Electronic Materials <https://doi.org/10.1002/aelm.201800591> , That has been published in its final form: <https://onlinelibrary.wiley.com/doi/abs/10.1002/aelm.201800591>
We found that under the same exposure conditions (temperature and H₂ concentrations) the response time of all produced devices is similar. We also found that the response time remains mostly unchanged for repeated measurements using the same device.

2. Reversibility and reproducibility of the I_{SD} x *Time* curves for H₂ exposure at 473 K

To investigate the reversibility and reproducibility of the H₂ reaction with the monolayer, we carried out long I_{SD} vs. *Time* measurements of the MoS₂ FET under 160 minutes exposure to 20 % H₂ at $V_G = -20$ V and temperature of 473 K, as shown in Figure S2. The red curve measurement was obtained right after the black curve, exhibiting only small changes in comparison with the first curve, probably due to experimental variations. These results indicate a good reproducibility of the device behavior. We observe a complete recovery in these conditions after 16 h in pure Ar.

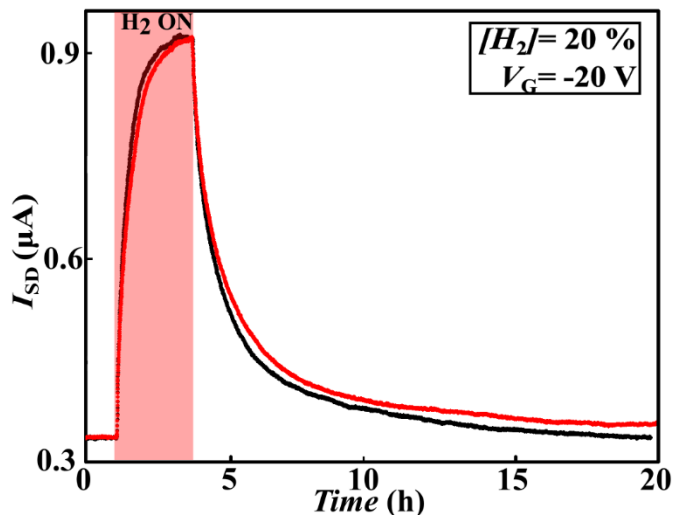


Figure S2: Source-drain current (I_{SD}) as a function of time for 160 min under 20 % H₂ exposure for MoS₂ FET at $V_G = -20$ V and 473 K. The red curve measurement was obtained immediately after the black curve measurement.

3. Raman study of structural changes in the MoS₂ FET due to the H₂ exposure

We searched for possible structural changes in the MoS₂ due to the H₂ exposure using Raman spectroscopy. The Raman spectra and maps were recorded using a WITec Alpha 300 system operating with a 532 nm excitation source at 0.5 mW power. To investigate the variations in the Raman spectra, we compare the spectra before and after the exposure of the MoS₂ to [H₂]= 65% at 473 K, during 6 h, as shown in Figure S3. The Raman spectra before the H₂ exposure are represented by blue curves in Figure S3a. The energy difference (Δ) between the E_{2g}¹ and A_{1g} modes present a fixed value of $\Delta= 19$ cm⁻¹, which is an accurate indicator of layer thickness for monolayer MoS₂.^[1] In the Figure S3b, we show a comparison of the spatially resolved Raman spectroscopy of E_{2g}¹ (top Figure) and A_{1g} (bottom Figure) modes before and after H₂ exposure. Both Raman spectra and maps were calibrated using the silicon peak after the H₂ exposure to reproduce the measurements. We do not observe relevant shifts in our experiments according to the precision of the measurement setup, of approximately 1 cm⁻¹.

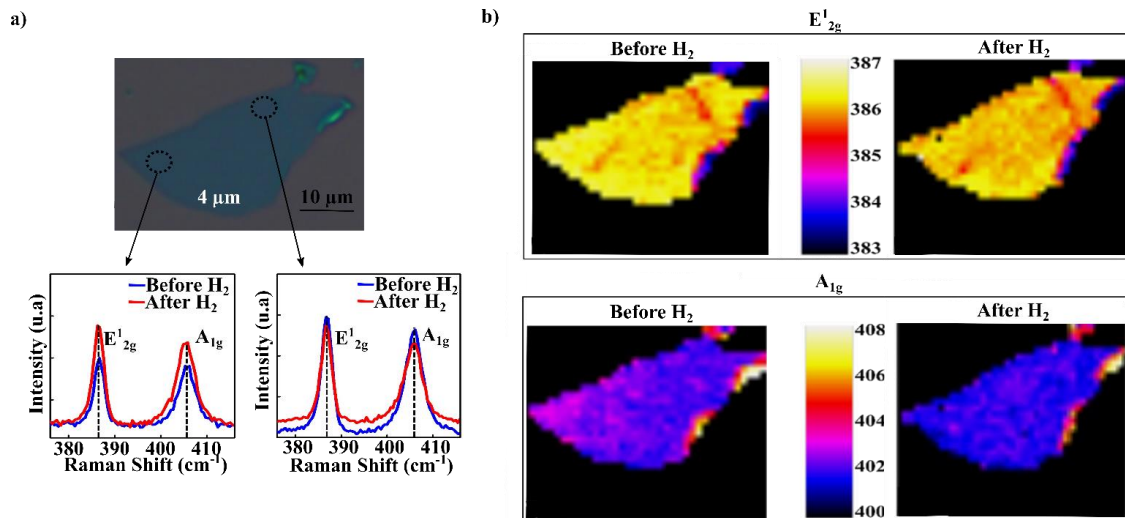


Figure S3: a) Raman spectra of the MoS₂ before and after the exposure to [H₂]= 65% at 473 K, during 6 h; b) Spatially resolved Raman spectroscopy of E_{2g}¹ and A_{1g} modes before and after H₂ exposure.

4. Four probe measurement configuration

Figure S4a and S4b show a sketch of the circuits for two and four probe configuration, respectively, considering the resistances that influence the measurements. As depicted in Figure S4a, when we carry out electric measurements using two terminals, the contact resistances are included in the total resistance of the device, since each contact is used to both apply current and measure the voltage. To avoid the effect of the contact resistance on the measurements, we performed measurements with four terminals, as shown in Fig. S4b. To carry out the four probe measurements, we used a Keithley K2400 source to applied a fixed DC current (I) of 1×10^{-6} A between the source (Sr) and drain (D) terminals. The voltage (V) between the internal terminals C_1 and C_2 (Figure S4b) was measured by a Keithley 2000 Digital Millimeter. A Keithley K2400 source was used to provide a DC gate voltage (V_G).

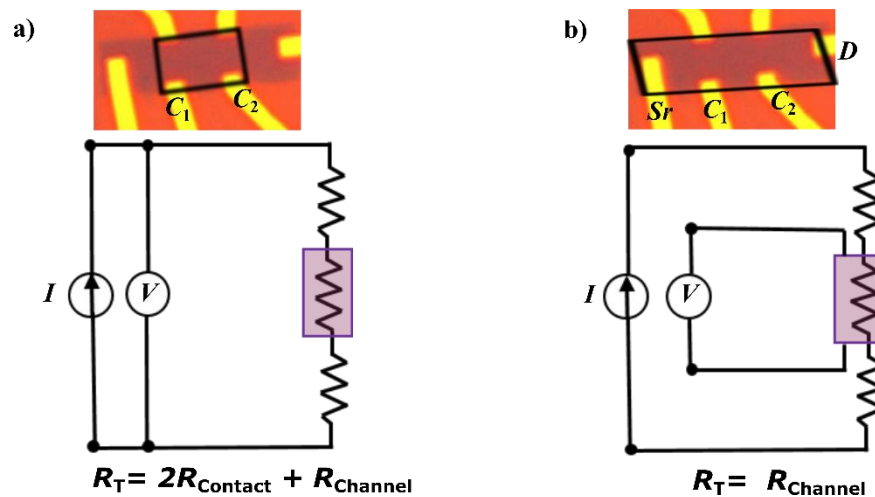
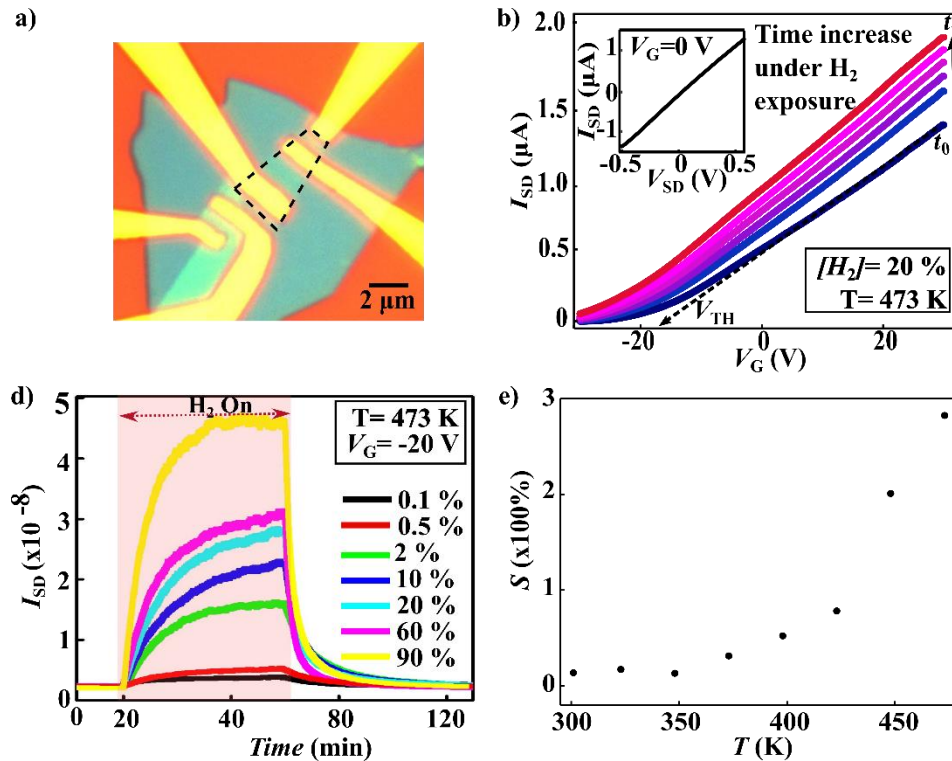


Figure S4: Schematic representation of the circuits for two (a) and four probe (b) configurations, considering the resistances that influence the electric measurements.

5. MoS₂ FET supported on h-BN under H₂ exposure

Similarly to the measurements that were carried out for the MoS₂ FET supported on SiO₂, we investigated the response of the MoS₂ FET supported on h-BN (Figure S5a) to the $[H_2] = 20\%$ at 473 K (Figure S5b). Also, we measured a wider range of concentrations, spanning from 0.1 to 90% of H₂, as shown in Figure S5c. We must emphasize here that the devices have the same response behavior as a function of temperature and H₂ concentration was observed for both substrates.



S5: Study of H₂ interaction with a MoS₂ FET supported on h-BN at 473 K and V_{SD} = 0.1 V. a) Optical image of a typical MoS₂/BN device; b) I_{SD} x V_G curves of the MoS₂/BN transistor under 20% of H₂ exposure. Inset: I_{SD} x V_{SD} curve for V_G = 0 V, before H₂ exposure; c) Current change versus time in different hydrogen concentrations in fixed V_G = -20 V; d) Sensor response of MoS₂ monolayer as a function of temperature: from 300 K up to 473 K. The data were taken at a fixed gate voltage V_G = -20 V.

6. Atomic layer deposition (ALD) of Al₂O₃ on MoS₂ devices

6.1- ALD technique and MoS₂/Al₂O₃ morphology

The atomic layer deposition (ALD) of Al₂O₃ consists of two processes. The first ALD treatment is carried out with 50 trimethylaluminum (TMA) pulses (the Al precursor), which react with available terminations (vacancies, edges and point defects) in MoS₂. Next, alternated cycles of TMA (0.015s) and H₂O (0.015s) were used (with 30 s purge time after each pulse) to obtain the MoS₂/Al₂O₃ FETs. The calibrated thickness produced for a single TMA/H₂O cycle is ~0.09 nm.^[2,3] During the growth-process of Al₂O₃ films, the substrate temperature was fixed at 423 K.

This is the authors' version (pre peer-review) of the manuscript: N R. Rezende et al, Advanced Electronic Materials <https://doi.org/10.1002/aelm.201800591> , That has been published in its final form: <https://onlinelibrary.wiley.com/doi/abs/10.1002/aelm.201800591>

In Figure S6 we show the AFM image before and after 100 cycles of Al₂O₃ grown on a monolayer MoS₂ to evidence the morphology of the oxide film. The Al₂O₃ film is highly non-uniform due to the preferential nucleation at edges and defects. The Al₂O₃ clusters grow in the shape of nanospheres, which can be explained by the low surface energy of monolayer MoS₂ due to the presence of few effective dangling bonds.^[3,4]

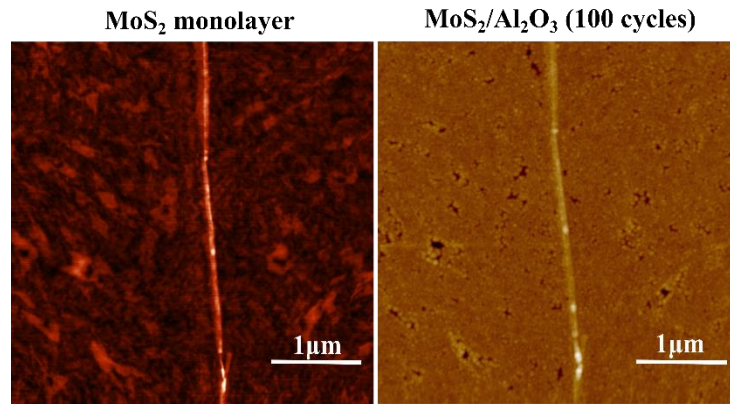


Figure S6: AFM image of the monolayer MoS₂ without Al₂O₃ and the MoS₂/Al₂O₃ hybrid structure

6.2- Mechanisms of adsorption and desorption of the H₂ in the MoS₂ FET

We believe that the fast increase in the current (region 1, in the **Figure S7a**) is explained by the reaction of H₂ with the top of the monolayer, while the longer time for the current saturation (region 2, in the **Figure S7a**) is explained by the diffusion of H₂ in between MoS₂ and the substrate. After the passivation of S vacancies in the MoS₂ with Al₂O₃ growth, both the response and recovery time increased due to the attenuation of fast adsorption and desorption mechanism at the top of the monolayer, as shown in **Figure S7b**.

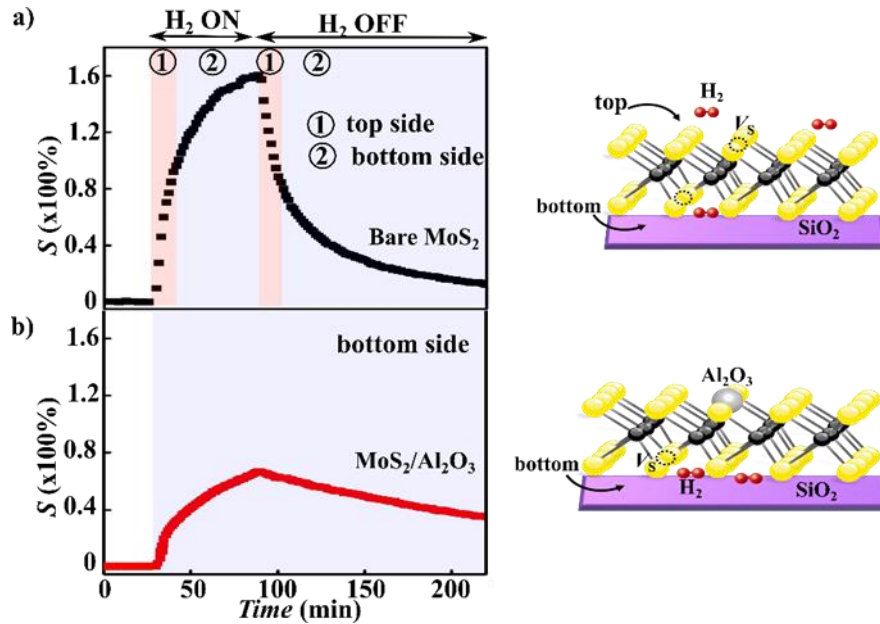


Figure S7: Sensor response as a function of time during the H_2 exposure, in fixed threshold voltage difference ($V_G - V_{\text{TH}} = 14$ V for the bare MoS_2 FET (a) and MoS_2 with 5 cycles of Al_2O_3 growth (b). The region 1 and 2 represent the interaction of H_2 with the top side and bottom side respectively. After the passivation of S vacancies in the MoS_2 with Al_2O_3 growth occurs the attenuation of fast adsorption mechanism at the top of the monolayer.

References

- [1] C. Lee, H. Yan, L. Brus, T. Heinz, J. Hone, S. Ryu, *ACS Nano* **2010**, *4*, 2695.
- [2] M. De Pauli, M. J. S. Matos, P. F. Siles, M. C. Prado, B. R. A. Neves, S. O. Ferreira, M. S. C. Mazzoni, A. Malachias, *J. Phys. Chem. B* **2014**, *118*, 9792.
- [3] Y. Li, X. Li, H. Chen, J. Shi, Q. Shang, S. Zhang, X. Qiu, Z. Liu, Q. Zhang, H. Xu, W. Liu, X. Liu, Y. Liu, *ACS Appl. Mater. Interfaces* **2017**, *9*, DOI 10.1021/acsami.7b08893.
- [4] S. Park, S. Y. Kim, Y. Choi, M. Kim, H. Shin, J. Kim, W. Choi, *ACS Appl. Mater. Interfaces* **2016**, *8*, 11189.